Investigations on supermolecular structure of poly(ethylene terephthalate) samples of higher modulus

D. Hofmann, U. Göschel, E. Walenta, D. Geiß and B. Philipp
Academy of Sciences of the German Democratic Republic, Institute of Polymer Chemistry 'Erich Correns', Teltow-Seehof, GDR-1530, GDR
(Received 1 March 1988; revised 7 July 1988; accepted 12 August 1988)

The supermolecular structure of higher modulus poly(ethylene terephthalate) (PET) samples obtained by means of multi-stage combined cold drawing/hot zone drawing procedures is characterized using WAXS, SAXS and mechanical methods. The direct separate determination of crystallite sizes and lattice distortions using a single line method has been applied for the first time to high modulus PET samples. Influences of supermolecular structure on the axial elastic modulus and on a limitation in preparing high modulus PET samples are discussed.

(Keywords: poly(ethylene terephthalate); supermolecular structure; wide-angle X-ray scattering; lattice distortions; axial elastic modulus)

INTRODUCTION

Uniaxially oriented PET fibres and film strips are widely used commercially. In this connection, there has been much effort to increase the tensile modulus and tenacity of such materials and to investigate their supermolecular structure. The preparation of high modulus ($E \gtrsim 10$ GPa) PET fibres often takes place via a combination of drawing and zone drawing with subsequent annealing or zone annealing[1-7]. There are also reports on the annealing of commercially produced PET fibres[8]. The modulus values given[1-8] do not significantly exceed 20 GPa in any instance. Only Casey[21] has reported Young's modulus values of 20–30 GPa for PET films which had been drawn near to the glass transition temperature with draw ratios greater than 3, but no detailed information about the determination of modulus was given. There are numerous publications about the supermolecular structure of highly orientated PET materials in general[9-36].

The present paper describes an investigation of the supermolecular structure of uniaxially orientated PET samples, which were obtained by a systematic variation of a zone drawing procedure developed by Marichin *et al.*[37,38] for PE fibres and modified by Göschel *et al.*[39] for the preparation of PET samples from amorphous precursors. In spite of extensive variation in the drawing parameters it was not possible to prepare PET samples with a Young's modulus above 20 GPa. It is one aim of this paper to discuss structural causes of this behaviour.

The supermolecular structure of the high modulus PET samples was determined from the orientation of molecular chains in the crystalline regions, the SAXS-long periods, the crystallinity and the axial modulus. So far as we know, and with one exception[21], lattice distortion parameters and crystallite size parameters are not allowed for in the literature. We used a single line method[40,41] to determine both the corrected number of average crystallite size values and the respective root mean square lattice strains. These structural parameters were correlated with the axial Young's modulus of the samples.

For the discussion of the structure of non-crystalline regions a Takayanagi model was used (see refs. 2, 3 and 25).

EXPERIMENTAL

Preparation of samples

Nearly isotropic ($\Delta n = 0.5 \times 10^{-3}$) and non-crystalline PET film strips ($M_w = 20\,000$) with a thickness of 180 μm and width 2.8 mm were used as precursors. The following method was chosen to obtain high modulus PET samples from them: in the first step a high level of uniaxial orientation of the molecular chains was achieved via a very slow ($V_d \leqslant 6$ mm min^{-1}) cold drawing stage below the glass transition temperature, T_g[42,43]. In a second step partial crystallization and further improvement of the high degree of molecular orientation was obtained by one or more hot zone drawing stages. The whole drawing process can be seen from the drawing scheme in *Figure 1*. The drawing conditions are listed in *Table 1*. The best drawing conditions for the first hot drawing stage were 433 K $\lesssim T_d \lesssim$ 473 K and 300 MPa $\lesssim \sigma \lesssim$ 400 MPa, and for the second 473 K $\lesssim T_d \lesssim$ 506 K and σ near 400 MPa. These parameters gave the most reliable drawing method and also the most acceptable mechanical properties.

X-ray investigations

Wide-angle X-ray scattering (WAXS) patterns were obtained for all samples using a vacuum flat film camera in perpendicular transmission. For all the semicrystalline samples the ($\bar{1}05$)-diffraction profile was measured from a symmetrical transmission goniometer scan. All

0032-3861/89/020242-06$03.00
© 1989 Butterworth & Co. (Publishers) Ltd.

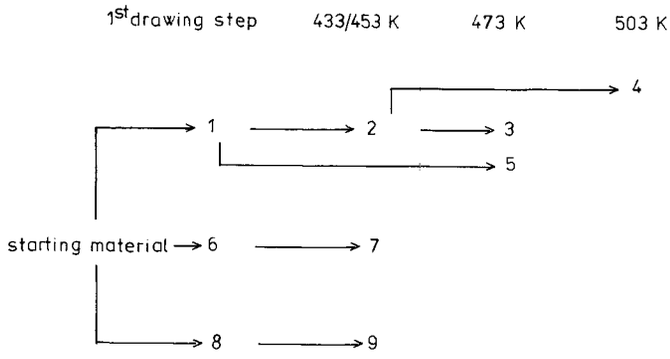

Figure 1 Drawing scheme

Table 1 Processing conditions for the PET samples

Sample	Processing conditions
1	Single step zone drawing with $T_d = 341$ K, $V_d = 5.5$ mm min^{-1}, $\sigma = 15$ MPa
2	As sample 1 plus zone drawing with $T_d = 433$ K, $V_d = 100$ mm min^{-1}, $\sigma = 70$–350 MPa (stepwise)
3	As sample 2 plus zone drawing with $T_d = 473$ K, $V_d = 100$ mm min^{-1}, $\sigma = 200$–370 MPa (stepwise)
4	As sample 2 plus zone drawing with $T_d = 503$ K, $V_d = 100$ mm min^{-1}, $\sigma = 200$–400 MPa (stepwise)
5	As sample 1 plus zone drawing with $T_d = 473$ K, $V_d = 100$ mm min^{-1}, $\sigma = 200$–400 MPa (stepwise)
6	Single step zone drawing with $T_d = 353$ K, $V_d = 100$ mm min^{-1}, $\sigma = 38$ MPa
7	As sample 6 plus zone drawing with $T_d = 433$ K, $V_d = 100$ mm min^{-1}, $\sigma = 70$–250 MPa (stepwise)
8	Single step drawing in a homogeneous temperature field with $T_d = 296$ K, $V_d = 3$ mm min^{-1}
9	As sample 8 plus zone drawing with $T_d = 453$ K, $V_d = 100$ mm min^{-1}, $\sigma = 100$ MPa
10	Single step zone drawing with $T_d = 313$ K, $V_d = 150$ mm min^{-1}

T_d, drawing temperature; V_d, drawing velocity; σ, tension of drawing

crystallites with the normals on the ($\bar{1}05$) lattice planes orientated in the drawing direction contributed to this profile. (The normals of the ($\bar{1}05$)-lattice planes show the smallest angle to the c-axis (8–10°)[30,44] of all resolvable WAXS-reflections of PET.)

The registration of the WAXS-profile of the (100)-peak was performed for crystallites with the normals on the (100)-lattice planes orientated in the T-direction. All diffraction profiles were measured with Ni filtered CuKα-radiation. The diffraction profiles were corrected for parasitic scattering, absorption, polarization and $CuK_{\alpha_1\alpha_2}$ doublet broadening. The background correction was done according to Vonk[45], where in the case of equatorial profiles the equatorial scattering curve of a highly orientated but non-crystalline cold-drawing product (see samples 1 and 8 in *Table 1*) was used as standard background (see *Figure 2*).

Separation of the overlapping reflections was performed via a Pearson-VII-function fit programme[46–48].

Finally, the WAXS-reflection profiles were corrected for instrumental broadening according to Stokes[49] using an anthracene standard specimen. From the fully corrected and resolved peak profiles the number average crystallite sizes L_{hkl} and the root mean square lattice strains $\sqrt{\langle e_i^2 \rangle}$ perpendicular to the corresponding scattering lattice planes were obtained by means of a single line method[40,41].

For the characterization of crystalline chain orientation an azimuthal goniometer scan of the ($\bar{1}05$)-reflection was made. From this the angular distance γ between the average orientation of the crystalline c-axes and the drawing direction was determined. The orientation factor f_c according to Stein[50] was calculated:

$$f_c = (3\langle \cos^2 \alpha' \rangle - 1)/2 \quad (1)$$

using the background correction of Gupta *et al.*[30] and the separation from the ($0\bar{2}4$) peak after Desai[33]. In equation (1) α' is determined from α (azimuthal angle measured from the equator) in such a manner that the maximum of intensity of the respective azimuthal scan will be positioned at $\alpha' = 0°$. Then, f_c is a measure for the scattering of orientation of the crystalline c-axes about the mean value characterized by γ.

The meridional long period L was determined for the SAXS flat film photographs. For the fibrillar morphology, L is the average length of a structural unit element composed of a crystallite and the adjoining non-crystalline region. In this connection the ratio ($L_{\bar{1}05}/L$) is the linear degree of order, which is a measure of the crystalline content. The linear degree of order is appropriate for the discussion of Takayagi models for the axial elastic behaviour of uniaxially drawn samples, if the investigated material possesses a fully fibrillar structure as is often assumed for highly oriented PET samples[13,17,19–21,26,34].

Mechanical investigations

For all samples the stress–strain curves were recorded quasi-statically at 296 K using an Instron tensile tester. Young's modulus was then calculated from these curves. Further mechanical properties such as the tensile strength will be discussed elsewhere[39].

RESULTS AND DISCUSSION

Cold drawn samples

Examination of the WAXS flat film photographs reveals that the slow cold drawn samples 1 and 8 are amorphous and have a high degree of orientation (see

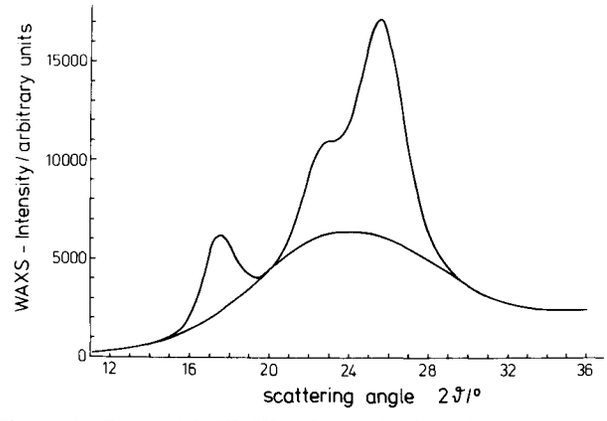

Figure 2 Equatorial WAXS of sample 9 with separation of background

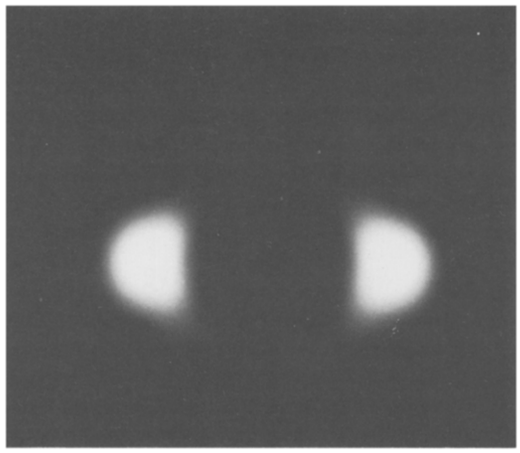

Figure 3 WAXS pattern of sample 1 (slow cold drawn)

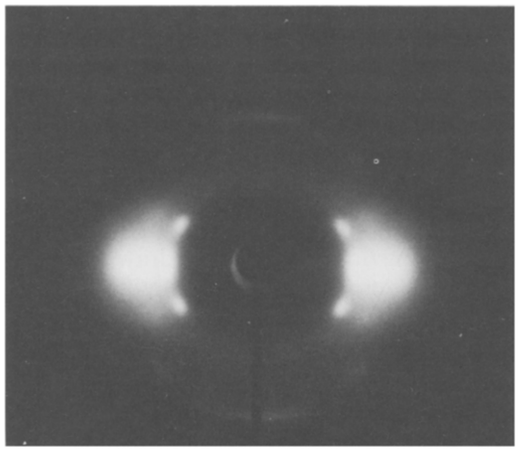

Figure 4 WAXS pattern of sample 10 (fast cold drawn)

Figure 3). These samples are almost transparent. The fast cold drawn sample 10 ($V_d = 150\,mm\,min^{-1}$) shows distinct crystalline WAXS-reflections together with a highly orientated non-crystalline halo (see *Figure 4*). Considering that the molecular orientation of samples 1, 8 and 10 are nearly equal, it can be concluded that the comparatively low modulus of sample 10 ($E = 3\,GPa$) does not result from orientation effects.

Sample 10 is opaque. According to Pakula and Fischer[24] this may be attributed to the presence of elongated shape cavities orientated in the direction of drawing. These might be one reason for the low modulus of this specimen.

A further interpretation of the different values of the Young's moduli of the three cold drawn samples may be as follows: according to Peterlin[51] the linear degree of order and the fraction of intrafibrillar taut tie molecules are closely related to the Young's modulus of semi-crystalline polymer samples with a highly orientated fibrillar morphology. But this modulus also depends on the density of chain ends and trapped molecular entanglements for non- or poorly crystalline material. Many more chains can be expected to rupture between entanglement points during very fast cold drawing (sample 10) than during very slow drawing (samples 1 and 8). Thus, sample 10 has fewer taut chain sections carrying the load than samples 1 and 8.

Crystalline regions of PET consist only of *trans* chain units, forming a triclinic crystalline lattice[52]. It can be assumed that there is an increasing tendency of the *gauche* conformation units in the unorientated amorphous starting product to be transformed into *trans* units concerning the crystallization, during cold drawing, of PET. This transformation thus causes a distinct alignment and orientation of molecular chains[26]. If such a state of molecular orientation is achieved only a small additional amount of energy is necessary to initiate a partial crystallization. Crystallization during cold drawing of PET is discussed as a result of the mechanical tensions acting on the molecules.

In order to obtain more information about the influence of thermal effects on crystallization during cold drawing of PET, Nitzsche and Hofmann[53] carried out a fast drawing of a PET sample in a homogeneous temperature field ($T_d = 313\,K$, $V_d = 600\,mm\,min^{-1}$, $\sigma \approx 25$–$30\,MPa$). Under those conditions a neck formation was observed. The WAXS flat film photograph of that material shows distinct crystalline reflections. For comparison a sample also drawn via neck formation at the same temperature very slowly ($V_d = 5\,mm\,min^{-1}$) was stressed after drawing statically with a tension $> 30\,MPa$.

The WAXS flat film photograph of that sample is of the same type as shown in *Figure 3*, i.e. no crystalline reflections are seen. In the case of fast drawing, therefore, it is obviously not the tension of drawing but the adiabatically increased temperature in the neck region of the sample which is the relevant parameter for crystallization.

HOT DRAWN SAMPLES

Supermolecular structure of the crystalline regions

In discussing the results obtained with hot drawn samples the triclinic symmetry of PET crystallites has to be taken into consideration. In this triclinic lattice the crystalline chain axes (*c*-axes) are not perpendicular to the (001)-lattice planes (boundaries between crystalline and non-crystalline sample regions in one fibril). Therefore, models of supermolecular structure based on the assumption that an average parallel orientation of crystalline chain axes occurs simultaneously with a perpendicular orientation of the (001)-lattice planes to the drawing direction[2,3,14,15,22,27,28], are less suited for the interpretation of our results. Suitable structural models can be subdivided into fibrillar models and models of a para-crystalline layer lattice. Casey[21] discussed a fibrillar model with oblique boundaries between non-crystalline and crystalline regions in a fibril with the crystalline *c*-axes showing a small inclination angle to the drawing direction. This inclination angle decreased with an increasing draw ratio λ and reached zero for higher λ values. Bonart[12,13], however, criticized fibrillar models for supermolecular structure of uniaxially oriented PET samples, which are connected with the assumption that no correlation exists between laterally adjoining fibrils. He supposed that in the case of highly oriented PET specimens laterally neighbouring crystalline regions often tend to form continuous crystalline layers. Biangardi and Zachmann[19,20] have further improved Bonart's considerations. For us, it is sufficient to consider a fibrillar model including some inclination of crystalline *c*-axes relative to the drawing direction without any further

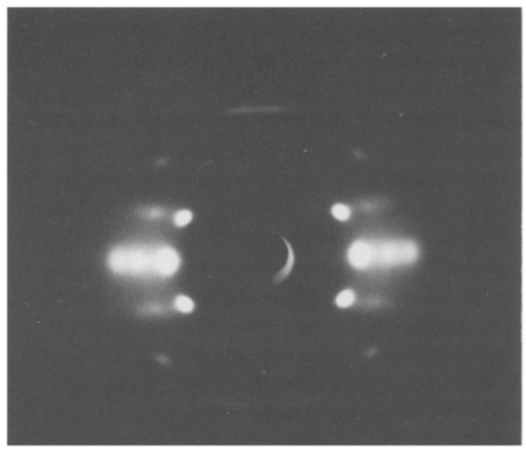

Figure 5 WAXS pattern of sample 3 (cold/hot zone drawn)

Table 2 Quantitative structure parameters for the PET samples

Sample	Reflection	γ	f_c	L_{hkl} (nm)	ε_1 (%)	L (nm)	$L_{\bar{1}05}/L$	E (GPa)
1	–	–	–	–	–	–	–	8.4
2	($\bar{1}$05)	0	0.98	3.8	2.6	14.5	0.26	13.4
	(100)			3.3	3.3			
	(010)			3.6	2.7			
3	($\bar{1}$05)	0	0.98	4.0	2.7	14.7	0.27	15.0
	(100)			3.4	2.9			
	(010)			3.9	2.3			
4	($\bar{1}$05)	0	0.98	5.1	2.9	15.7	0.33	16.8
	(100)			2.6	2.1			
	(010)			5.1	2.9			
5	($\bar{1}$05)	0	0.98	4.1	2.2	14.7	0.28	14.3
	(100)			2.7	2.0			
	(010)			4.5	2.4			
6	($\bar{1}$05)	–	0.87	4.2	2.2	14.8	0.28	7.1
	(010)			2.5	2.9			
7	($\bar{1}$05)	0	0.96	4.0	2.6	14.9	0.27	10.2
	(010)			2.9	2.1			
8	–	–	–	–	–	–	–	10.2
9	($\bar{1}$05)	0	0.98	5.0	2.4	12.7	0.39	15.0
	(100)			2.5	3.2			
	(010)			4.4	2.6			
10	–	–	–	–	–	–	–	3.0

γ, inclination angle between average crystalline chain direction and drawing direction; f_c, orientation factor after Stein[50]; L_{hkl}, number average crystallite size; ε_1, per cent root mean square lattice strain; L, meridional SAXS-long period; ($L_{\bar{1}05}/L$), linear degree of order; E, quasistatically measured Young's modulus

specification. The WAXS flat film photographs of all hot zone drawn samples indicate a highly preferred orientation of the crystalline chains parallel to the drawing direction (see *Figure 5*). Furthermore, these specimens should have a significantly higher crystallinity than the very fast cold drawn sample 10, for instance (see *Figure 4*). The quantitative results are shown in *Table 2*. All two- and three-steps-drawn samples have a nearly perfect orientation of the *c*-axes parallel to the draw direction. Therefore, the observed differences in modulus up to 65% (see sample 7, $E=10.2$ GPa; sample 4, $E=16.8$ GPa) cannot have been caused by differences in crystalline orientation. For sample 6, however, which was single-step drawn at T_g, a certain deviation of the average *c*-axis orientation relative to the draw direction ($\gamma=7°$) connected with a greater scattering ($f_c=0.87$) should be mentioned. Both effects vanished after subsequent hot drawing stage (sample 7). All orientation parameters in *Table 2* are within the range given in the literature for higher modulus PET samples ($\gamma=0$ ... 8°, $f_c=0.87$ ... 0.99)[1-3,5,21].

All these materials show longitudinal crystallite sizes ($L_{\bar{1}05}=3.5$ ... 5.1 nm) comparable with those listed in the literature[1,18,23], whereas the lateral crystallite sizes were slightly smaller[1,8]. They indicate a non-circular cross-section for the fibrils (see also refs. 1 and 34). The deviation from a circular cross-section is greater the lower the drawing tension in the second drawing stage (see sample 9), and the higher the drawing temperature in the third drawing step (see samples 4 and 5).

A clear correlation between the crystallite size and the axial Young's modulus was not found. Only the two specimens with the lowest elastic moduli (samples 6 and 7) show L_{010} values distinctly smaller than those with the higher modulus materials.

As far as we know, only Casey[21] has dealt with a somewhat rough estimation of crystalline lattice distortions in chain direction. In his study, the Hosemann g_{II} parameter, which is comparable to our ε_1 parameter, was determined via a two-line method from the broadening of the ($\bar{1}$03)- and the ($\bar{1}$05)-reflections. The ($\bar{1}$03) peak was assumed to be third order, and the ($\bar{1}$05) peak to be fifth order for the same set of lattice planes. Casey obtained g_{II} values between 0.6% and 0.9% for his higher modulus PET samples. These values are well below our ε_1 values. In our opinion, one reason for this discrepancy is that Casey arbitrarily defines two reflections of first order as peaks of third and fifth order. However, with the Hosemann paracrystal theory[54], the lattice distortions g_{II} determined from a reflection with a given broadening will be smaller the higher the order its reflection is assumed to be.

The lattice distortion parameters ε_1 listed in *Table 2* do not show any essential differences between the individual samples. There is no direct correlation between the Young's moduli of the specimens and the lattice distortions.

Young's modulus and supermolecular structure

Knowledge about orientation, size and perfection of the crystallites, which can be obtained by WAXS, is obviously not sufficient for the discussion of the correlations between the axial elastic modulus under small strains and the supermolecular structure of the investigated PET samples. In this connection the structure of non-crystalline regions is highly important. In this case the Young's moduli are mainly determined by the fraction of taut (i.e. all *trans*) tie molecules between crystallites in the same fibril. These molecules connect crystallites which are neighbours in one fibril through a non-crystalline region, and have the same axial modulus as a chain section in a crystallite. In addition, the amount of crystalline (i.e. highly stiff) material along a fibril is important for the Young's modulus. This amount can be quantified by the linear degree of order ($L_{\bar{1}05}/L$). For an approximately quantitative description of the influence of the linear degree of order and the average fraction β of taut tie molecules on the Young's modulus Peterlin[51] proposed a simple series–parallel model of a structural unit element for uniaxially orientated polymer samples (see *Figure 6*). Assuming a uniform distribution of taut tie molecules over the cross-section of the non-crystalline

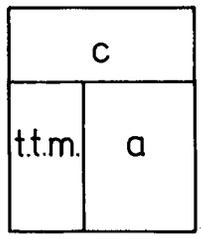

Figure 6 Series parallel model for a structural unit element after Peterlin[51]. t.t.m., taut tie molecules; a, non-stretched molecular proportion of a non-crystalline region; c, crystalline material

Table 3 Fraction of taut tie molecules for the hot zone drawn PET products

Sample	E/E_c	$(L_{\bar{1}05}/L)$	β
2	0.122	0.26	0.093
3	0.136	0.27	0.103
4	0.153	0.33	0.108
5	0.130	0.28	0.097
7	0.093	0.27	0.069
9	0.109	0.39	0.070

regions, the following equation for the axial Young's modulus E is valid, if $(L_{\bar{1}05}/L)$ is used as the linear degree of order (see ref. 51).

$$E = E_c(\beta + (1-\beta)E_a/E_c)/(1-(L_{\bar{1}05}/L)(1-\beta)(1-E_a/E_c)) \quad (2)$$

E_a is the axial modulus of a completely amorphous sample and E_c the axial modulus of a single crystal specimen. Provided $E_a \ll E_c$ and knowing E and $(L_{\bar{1}05}/L)$, the fraction β of taut tie molecules can be estimated as follows[51]:

$$\beta = E(1-(L_{\bar{1}05}/L))/(E_c(1-E(L_{\bar{1}05}/L)/E_c)) \quad (3)$$

Two further prerequisites for the validity of (3) should be mentioned. First affine deformations have to be assumed, i.e. that the longitudinal tensions and strains acting on the whole sample are the same as those acting on a single structural unit element. Secondly lateral mechanical interactions between adjoining fibrils are negligible.

With (3) the fraction β of taut tie molecules was estimated for the hot zone drawn samples. A mean value of E_c ($E_c = 110$ GPa) was used[10,25,55,56]. The $(L_{\bar{1}05}/L)$ values in *Table 3* are within the crystallinity range given in the literature for highly oriented PET samples[1,3,8,18,23,25].

Table 3 shows that the samples 2, 3, 5 and 7, which are comparable with reference to their linear degrees of order and their uniaxial orientation, differ in the fraction (β) of taut tie molecules. This fraction β, and therefore the axial elastic modulus, increase with an increasing number of drawing steps (see samples 1, 2, 3) and with a decreasing crystallinity of the highly orientated intermediate product of the first drawing step (see samples 2 and 7 which were produced under nearly identical conditions of the second drawing stage).

Every drawing of a semi-crystalline product can result in the breaking of tie chains, which were taut before this drawing, and in stretching of tie molecules, which were not taut before drawing.

If these opposing processes cause an increase of the fraction β of taut tie molecules the axial Young's modulus will increase. Therefore, semi-crystalline samples with axial elastic moduli near the maximum value E_c should contain many tie molecules in the non-crystalline regions. Furthermore, these tie molecules must have a length distribution as sharp as possible and with the maximum of this distribution close to the length of a tie molecule, which is taut even for very small strains. Additionally, the axial modulus may rise by an increase of crystallinity (see samples 4 and 9).

CONCLUSIONS

The axial elastic behaviour of high modulus uniaxially orientated PET samples depends on their supermolecular structure in a complex manner.

There seems to be no distinct correlation between Young's modulus on the one hand and crystallite sizes and lattice distortions on the other hand. Furthermore, the results discussed above show that for the non-crystalline as well as for the semi-crystalline uniaxially drawn PET samples a highly preferred orientation of molecular chain axes is necessary, but not a sufficient condition for obtaining high modulus.

The axial Young's modulus decisively depends on the fraction and length distribution of intrafibrillar tie molecules and the degree of crystallinity.

Notwithstanding the extensive variation of drawing parameters, it was not possible to produce samples with an axial Young's modulus higher than $\approx 15\%$ of the maximum value E_c. This is connected with the following problems: usually the preparation of high modulus PET samples starts with a material quenched from the melt. Such materials possess a much higher density of chain entanglements than, for instance, gel drawn very high modulus PE fibres (see, e.g. refs. 57 and 58).

Additionally, connected with the relatively low molecular weight of the PET materials used here, the density of chain ends is very high. Finally, the PET molecule has a complex structure.

All these problems contribute to the essentially lower crystallinity of higher modulus PET samples compared with high modulus PE materials. The high chain end density in the PET materials lowers the whole content of intrafibrillar tie molecules. It may be possible that here the total amount of tie molecules is not much higher than $\approx 10\%$. This means that the content of taut tie molecules cannot be increased above the same limit using drawing procedures.

Furthermore, drawing may cause a stretching of tie molecules, which were not taut before the respective drawing step, and a breaking of tie chains, which were taut before. Altogether it seems to be impossible to achieve a sufficiently high level of crystallinity and content of taut tie molecules simultaneously using the methods which up to now have been known for the production of higher modulus PET samples. Consequently there seems to exist a certain limitation for both the multi-stage drawing procedure discussed here and the methods of high modulus PET samples preparation reported in the literature.

REFERENCES

1 Sibilia, J. P., Harget, P. J. and Tirpak, G. A. *Polym. Prep.* 1974, **15**, 1
2 Kunugi, T., Suzuki, A. and Hashimoto, M. *J. Appl. Polym. Sci.* 1981, **26**, 213
3 Kunugi, T., Suzuki, A. and Hashimoto, M. *J. Appl. Polym. Sci.* 1981, **26**, 1951
4 Kunugi, T., Ichinose, C. and Suzuki, A. *J. Appl. Polym. Sci.* 1986, **31**, 429
5 Abhiraman, A. S. and Song, J. W. *J. Polym. Sci., Polym. Lett. Edn.* 1985, **23**, 613
6 Amano, M. and Nakagawa, K. *Polymer* 1986, **27**, 1483
7 Yoon, K. J., Desai, J. P. and Abhiraman, A. S. *J. Polym. Sci., Polym. Phys. Edn.* 1986, **24**, 1665
8 Jeziorny, A. *Acta Polym.* 1986, **37**, 137
9 Dulmage, W. L. and Contois, L. E. *J. Polym. Sci.* 1958, **28**, 275
10 Dulmage, W. J. and Geddes, A. L. *J. Polym. Sci.* 1958, **31**, 499
11 Bonart, R. *Kolloid Z.-Z. Polym.* 1964, **199**, 136
12 Bonart, R. *Kolloid Z.-Z. Polym.* 1966, **213**, 1
13 Bonart, R. *Kolloid Z.-Z. Polym.* 1969, **231**, 438
14 Dismore, P. F. and Statton, W. O. *J. Polym. Sci.* 1966, **C13**, 133
15 Koenig, J. L. and Hannon, M. J. *J. Macromol. Sci., Phys.* 1967, **B1**, 119
16 Prevorsek, D. C., Harget, P. J., Sharma, P. K. and Reimschuessel, A. C. *J. Macromol. Sci., Phys.* 1973, **B8**, 127
17 Güllemann, H. *Melliand Textilber. Int.* 1972, **53**, 910
18 Fischer, E. W. and Fakirov, S. *J. Mater. Sci.* 1976, **11**, 1041
19 Biangardi, H. J. and Zachmann, H. G. *Progr. Colloid Polym. Sci.* 1977, **62**, 71
20 Biangardi, H. J. *Makromol. Chem.* 1978, **179**, 2051
21 Casey, M. *Polymer* 1977, **18**, 1219
22 Misra, A. and Stein, R. S. *J. Polym. Sci., Polym. Phys. Edn.* 1979, **17**, 235
23 Nitzsche, K. and Vettegren, V. I. *Acta Polym.* 1979, **30**, 302
24 Pakula, T. and Fischer, E. W. *J. Polym. Sci., Polym. Phys. Edn.* 1981, **19**, 1705
25 Bower, D. I., Korybut-Daszkiewicz, K. K. P. and Ward, I. M. *J. Appl. Polym. Sci.* 1983, **28**, 1195
26 Pereira, J. R. C. and Porter, R. S. *J. Polym. Sci., Polym. Phys. Edn.* 1983, **21**, 1132
27 Pereira, J. R. C. and Porter, R. S. *J. Polym. Sci., Polym. Phys. Edn.* 1983, **21**, 1147
28 Pereira, J. R. C. and Porter, R. S. *Polymer* 1984, **25**, 869
29 Pereira, J. R. C. and Porter, R. S. *Polymer* 1984, **25**, 877
30 Gupta, V. B., Ramesh, C., Patil, N. B. and Chidambareswaran, R. K. *J. Polym. Sci., Polym. Phys. Edn.* 1983, **21**, 2425
31 Wakelyn, N. T. *J. Appl. Polym. Sci.* 1983, **28**, 3599
32 Brown, D. J. *Polym. Commun.* 1985, **26**, 42
33 Desai, P. and Abhiraman, A. S. *J. Polym. Sci., Polym. Phys. Edn.* 1985, **23**, 653
34 Scherz, D. and Heinrichsen, G. *Colloid Polym. Sci.* 1985, **263**, 975
35 Petermann, J. and Rick, U. *J. Polym. Sci., Polym. Phys. Edn.* 1987, **25**, 279
36 Rao, M. V. S. and Dweltz, N. E. *J. Appl. Polym. Sci.* 1987, **33**, 835
37 Marikhin, V. A., Mjasnikova, L. P. and Pelzbauer, Z. *Macromol. Sci., Phys.* 1983, **B22**, 111
38 Marikhin, V. A., Mjasnikova, L. P., Zenke, D., Hirte, R. and Weigel, P. *Vysokomol. Soed.* 1984, **24**, 210
39 Göschel, U. *Acta Polym.* in press
40 Hofmann, D. and Walenta, E. *Polymer* 1987, **28**, 1271
41 Hofmann, D., Fink, H.-P. and Philipp, B. *Polymer* 1989, **30**, 237
42 Göschel, U., Marikhin, V. A. and Mjasnikova, L. P. DD-PS 244 262 (1.4.87)
43 Göschel, U., Marikhin, V. A. and Mjasnikova, L. P. DD-WP B 29 B, 308 901 (11.11.87)
44 Jungnickel, B.-J. *Angew. Makromol. Chem.* 1984, **125**, 121
45 Vonk, C. G. *J. Appl. Cryst.* 1973, **6**, 148
46 Heuvel, H. M., Huisman, R. and Lind, K. C. J. B. *J. Polym. Sci., Polym. Phys. Edn.* 1976, **14**, 921
47 Fink, H.-P., Fanter, D. and Philipp, B. *Acta Polym.* 1985, **36**, 1
48 Walenta, E., Janke, A., Hofmann, D., Fanter, D. and Geiß, D. *Acta Polym.* 1986, **37**, 557
49 Stokes, A. R. and Wilson, A. J. C. *Proc. Phys. Soc.* 1949, **56**, 174
50 Stein, R. S. *J. Polym. Sci.* 1958, **31**, 327
51 Peterlin, A. in 'Ultra High Modulus Polymers' (Eds. A. Ciferri and I. M. Ward), Applied Science Publishers, London, 1979
52 Daubeny, R. de P., Bunn, C. W. and Brown, C. J. *Proc. R. Soc. (London)* 1954, **A226**, 531
53 Nitzsche, K. and Hofmann, D. unpublished results
54 Hosemann, R. and Bagchi, S. N. 'Direct Analysis of Diffraction by Matter', North-Holland Publ. Co., Amsterdam, 1962
55 Sakurada, I., Ito, T. and Nakamae, K. *Bull. Inst. Chem. Res.* Kyoto University 1964, **42**, 77
56 Sakurada, I. and Kaji, K. *J. Polym. Sci.* 1970, **C31**, 57
57 Kalb, B. and Pennings, A. J. *J. Mater. Sci.* 1980, **15**, 2584
58 Walenta, E., Hofmann, D. and Zenke, D. *Acta Polym.* accepted